



Photocatalytic degradation of rhodamine B and methylene blue by electrochemically prepared nano titanium dioxide/reduced graphene oxide/poly (methyl methacrylate) nanocomposite

Masoomeh Torabi Momen¹ · Farideh Piri¹ · Ramin Karimian²

Received: 4 October 2019 / Accepted: 22 January 2020 / Published online: 28 January 2020
© Akadémiai Kiadó, Budapest, Hungary 2020

Abstract

Composite of electrochemically prepared nano titanium dioxide/reduced graphene oxide/poly (methyl methacrylate) has been successfully synthesized. The homogeneous titanium dioxide nanoparticles (TiO₂ NPs) and reduced graphene oxide were prepared individually and composites of titanium dioxide nanoparticles/reduced graphene oxide (TiO₂/RGO) in different ratios were then prepared under sonication. Nano titanium dioxide/reduced graphene oxide/poly(methyl methacrylate) (TiO₂/RGO/PMMA) composite were prepared subsequently. The composites were characterized by X-ray diffraction (XRD), Fourier-transform infrared spectroscopy (FTIR), transmission electron microscopy (TEM), scanning electron microscopy (SEM) and electron dispersive spectrometer (EDS) for elemental analysis. Due to the long and great research interest as well as importance of developing new and efficient techniques in dyes degradation, methylene blue (MB) and Rhodamine B (RhB) were selected as two candidate to examine photocatalytic performance of the composites under 15 W UV-C lamp irradiation. Recovery of the TiO₂/RGO/PMMA composite also revealed slight decrease in photocatalytic performance after four cycles.

Keywords Nano titanium dioxide · Electrolytes · Sonication · Composites · Dye degradation · UV irradiation

Electronic supplementary material The online version of this article (<https://doi.org/10.1007/s11144-020-01722-x>) contains supplementary material, which is available to authorized users.

✉ Masoomeh Torabi Momen
m.torabi@znu.ac.ir

¹ Department of Chemistry, Faculty of Science, University of Zanjan, P.O. Box 45371-38791, Zanjan, Iran

² Chemical Injuries Research Center, Systems Biology and Poisonings Institute, Baqiyatallah University of Medical Sciences, Tehran, Iran

Introduction

Dyes and colorant are routinely used in many different industries. Currently, it is estimated that about 10–15 percent of the total produced dye is lost during he dyeing processes [1]. Since dyes are stable to light and oxidizing agents, many physical and chemical methods for their removal have proven to be unsuccessful [2]. Development of effective methods for dye removal is still an ongoing challenge. There has been growing interest in applying advanced oxidation processes (AOPs) as an efficient and applicable method for the complete degradation of different dyes in aqueous media [3–5]. Advanced oxidation processes include photocatalysts, ultraviolet or visible light irradiation and oxidants. The reaction proceeds by reactive species such as hydroxyl radicals ($\cdot\text{OH}$) and superoxide anion (O_2^-), which are generated when a semiconductor is in contact with water and oxygen and absorbs radiation, and will lead to quick and non-selective oxidation of a broad range of dyes [6] and organic pollutants [7, 8].

Among different photocatalysts, titanium dioxide is the most popular. Titanium dioxide is a promising semiconductor, which exists in three crystalline forms; anatase, rutile and brookite, with band gaps of 3.2, 3.02, and 2.96 eV for the anatase, rutile and brookite phases [9, 10]. Due to high physical and chemical stability of TiO_2 in alkaline and acidic conditions [11], high photocatalytic activity, chemical and photo stability, reusability, availability, nontoxicity, rather low cost and fast electron transfer to molecular oxygen, this semiconductor has been widely researched [12, 13]. Beside the different advantages of TiO_2 , which have made it a popular candidate in different research areas, there is a drawback that can partly limit its applications. Due to rather wide band gap of titanium dioxide, it mainly absorbs ultraviolet irradiation in the range shorter than 387 nm. Since UV light in solar light is less than 5%, this can lower the efficiency of titanium dioxide when sunlight is applied as the source of energy. Hence, great effort has been focused on developing new titanium dioxide based photocatalyst with efficient photoresponse in the range of visible light [14–19]. Besides, due to the rapid recombination rate of photo generated electron–hole pairs within TiO_2 particles, the photocatalytic efficiency on a bare TiO_2 remains limited. Recently, graphene based semiconducting nanocomposite made a way for solving the problems of electron–hole recombination and shows acceptable affinity towards photocatalytic reactions of TiO_2 NPs. The graphene layers adhere to TiO_2 NPs retrieve the induced electrons for photocatalytic reactions and prevent recombination with the photo generated holes [20, 21]

There are various reports on dyes degradation by nano titanium dioxide/graphene composites, including photocatalytic decolorization of methylene blue by silver loaded P25 TiO_2 /RGO [22], degradation of rhodamine B by composite of reduced graphene oxide/ TiO_2 composite films [23], congo red and methylene blue degradation by biphasic TiO_2 nanoparticles and its graphene nanocomposite [24] and degradation of many other dyes including reactive brilliant red and reactive orange 16 [25], amaranth azo dye [26]. To the best of our knowledge little work has been done on photocatalytic degradation of dyes by nano titanium dioxide/

poly (methyl methacrylate) composites, for instance decolorization of the methylene blue [27] photo degradation of phenol and methyl orange [28, 29], bleaching of methylene blue [30].

In the present study, we report modification of electrochemically prepared nano titanium dioxide with RGO and PMMA. The structural properties of the prepared composites were characterized using XRD, FTIR, SEM, EDS and TEM. The synthesized composites were applied for photocatalytic degradation of RhB and MB in aqueous solution.

Materials and methods

Reagents and apparatus

All chemicals including Sulfuric acid (H_2SO_4), nitric acid (HNO_3), tetra propyl ammonium bromide ($(\text{C}_3\text{H}_7)_4\text{NBr}$), Crystalline poly(methyl methacrylate) $[\text{CH}_2\text{C}(\text{CH}_3)(\text{CO}_2\text{CH}_3)]_n$, acetone ($\text{C}_3\text{H}_6\text{O}$), acetonitrile (CH_3CN), tetrahydrofuran (THF), toluene (C_7H_8), ethanol ($\text{C}_2\text{H}_5\text{OH}$), rhodamine B ($\text{C}_{28}\text{H}_{31}\text{ClN}_2\text{O}_3$), methylene blue ($\text{C}_{16}\text{H}_{18}\text{ClN}_3\text{S}$), platinum foil, (thickness 1.0 mm, 99.99% trace metals basis) and graphite rod (diameter 6 mm, 99.995% trace metals basis) were purchased from Sigma-Aldrich chemical suppliers and were used as received.

The commercially pure titanium (grade 2) with diameters of 5 mm in the shape of cylindrical bar was purchased from Shanghai Lushi metal materials limited company. The TiO_2 nanoparticle and prepared composites were characterized by various techniques including scanning electron microscopy equipped with electron dispersive spectrometer (SEM–EDS, MIRA III-TESCAN Company) and transmission electron microscopy (TEM, CM-120). A Fourier transform infrared spectrophotometer (FT-IR, Nicolet iS 10). X-ray diffraction (XRD-X'Pert Pro) with a scan range of 5° – 75° . Optical measurements were carried out on spectronic Helios Alpha Double-beam UV–VIS scanning spectrophotometers. Ultra sound bath (Bandelin, DT 102 H) was utilized for dispersion and preparation of the composites.

Preparation of titanium dioxide nanoparticles and reduced graphene oxide

Titanium dioxide nanoparticles were synthesized by an electrochemical method as follows [31]. Commercially available titanium rods with diameters of 5 mm were cut, mechanically polished and then cleaned and degreased by sonicating in individual solutions of acetone, ethanol and nitric acid for 10 min at room temperature and subsequent rinsing with deionized water. In the overall process, the bulk metal is oxidized at the anode, the metal cations migrate to the cathode and reduction takes place with formation of metal or metal oxide. Generally, the reactions were performed under agitation conditions by magnetic stirring in an open system. The two electrodes (titanium rod was used as anode and a piece of platinum foil was used as cathode) were placed parallel to each other in 3 cm apart connected to a DC power supply under a constant 30 V anodic potential and were immersed in 100 mL

of tetra propyl ammonium bromide (0.01 M) in acetonitrile/tetrahydrofuran (4:1) as the supporting electrolyte. The obtained nanoparticles were centrifuged and washed with THF to remove excess tetra propyl ammonium bromide and subsequently with distilled water at 5000 rpm (3×10 min). The preparation of reduced graphene oxide (RGO) was followed by electrochemical exfoliation process [32]. Briefly, a graphite rod (anode) and platinum foil (cathode) were immersed in 0.5 M of sulfuric acid solution as electrolyte. Electrochemical exfoliation process continued for 2 h by applying DC bias on graphite electrode at 10 V potentials. The samples were centrifuged and washed with deionized water several times then sonicated for 1 h and dried at 50 °C.

Preparation of titanium dioxide composites with RGO and PMMA

TiO₂/RGO composite were prepared by adding varied amount of TiO₂ to 5 mg of RGO to get 1/40, 1/60, 1/80, 1/100, 1/120, 1/140, 1/160 and 1/180 w/w ratios. The samples were grinded and mixed with a mortar and a blade then sonicated in a solution of absolute ethanol-deionized water (1:2) and dried subsequently. As shown in Fig. S1, RGO adding caused gradual change in TiO₂ white color. In order to obtain TiO₂/RGO/PMMA composite, different amount of Poly (methyl methacrylate) were dissolved in toluene, TiO₂/RGO (1/180 w/w) composite were then added and sonicated for 45 min. the final composites were obtained by evaporating the solvent.

Results and discussion

The FT-IR spectrum of nano TiO₂ powder is shown in Fig. S2a. A broad peak at 3356 cm⁻¹ and a sharp peak at 1617 cm⁻¹ is related to stretching vibrations of O–H and bending vibrations of adsorbed water molecules respectively and the broad intense peak at 903.79 cm⁻¹ is due to Ti–O–Ti vibration [33, 34], as it is shown in Fig. S2b, due to minute amount of added reduced graphene oxide, great changes in peaks is not observed. Reduced graphene oxide adding formed vivid peak in 1438 cm⁻¹ due to C–C stretching vibrations and minute changes in broad peak of 3356 cm⁻¹ and peaks below 1000 cm⁻¹. In TiO₂/RGO/PMMA spectrum, Fig. S2 c, the peak at 1731 cm⁻¹ is due to the C=O stretching vibration. The peak at 1447 cm⁻¹ is due to the C–H bending and the peaks around 1200 cm⁻¹ originate from the C–O stretching of the ester group.

Fig. 1 shows the FESEM images of the TiO₂ nanoparticles (a), TiO₂/RGO (b) and TiO₂/RGO/PMMA (c) nanocomposite. It can be clearly seen that titanium dioxide nanoparticles are in uniform distribution and rather spherical morphology with slight agglomeration which is due to rather long time gap over preparation of the desired samples and image taking. In order to get better insight of the structures, extra FESEM images of the composites are also added to supplementary material file (Fig. S3). TiO₂/RGO in 5 μm and 500 nm (b-1 and b-2), TiO₂/RGO/PMMA (c-1 and c-2) in 1 μm and 500 nm.

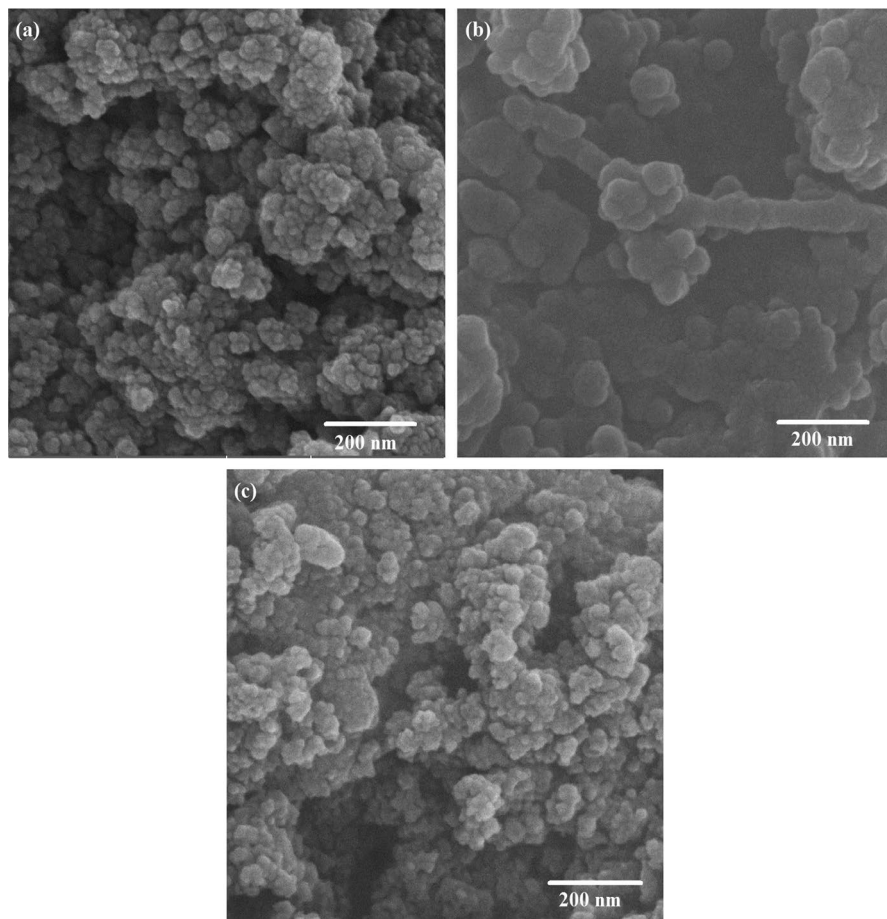


Fig. 1 FESEM images of TiO_2 (a), TiO_2/RGO (b) and $\text{TiO}_2/\text{RGO}/\text{PMMA}$ (c)

Transmission electron microscopy technique was also used to get better insight of the size and morphology of TiO_2 nanoparticles (Fig. 2)

EDS spectrums of the TiO_2 (a), TiO_2/RGO (b) and $\text{TiO}_2/\text{RGO}/\text{PMMA}$ (c) is shown in Fig. S4. Existence of expected atoms can be confirmed by EDS analysis. In EDS map of TiO_2 only titanium and oxygen peaks exist S4a, while in Fig. S4b and S4c vivid carbon peaks and increase in oxygen weight percent confirms existence of reduced graphene oxide and poly(methyl methacrylate). More weight percent of the carbon atom in $\text{TiO}_2/\text{RGO}/\text{PMMA}$ than TiO_2/RGO composite is also due to the addition poly(methyl methacrylate).

Fig. 3 shows the X-ray diffraction (XRD) patterns of TiO_2 (a) and TiO_2/RGO (b). It can be seen that native titanium dioxide nanoparticles with no annealing in furnace, showed rather crystalline nature with 2θ peaks at 25.6° , 38.3° , 47.8° , 54.6° , 62.9° , 69.2° and 75.3° , which coincides with 04-0477 standard and confirms

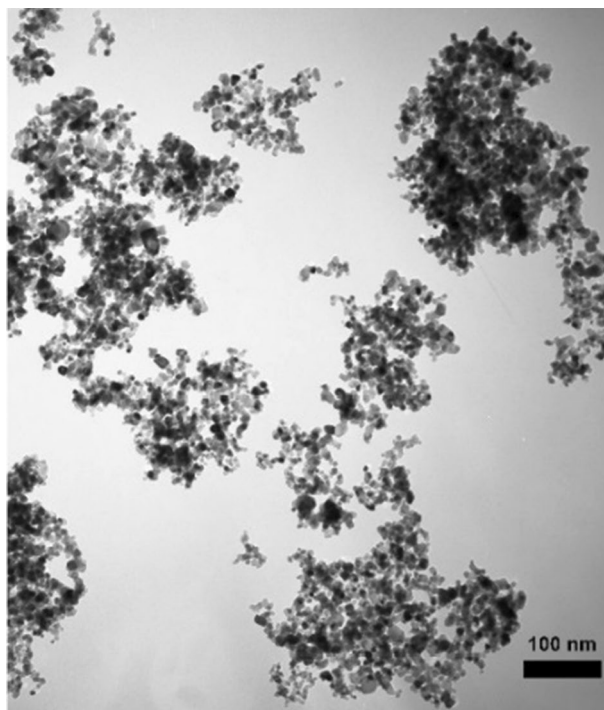


Fig. 2 TEM image of titanium dioxide nanoparticles

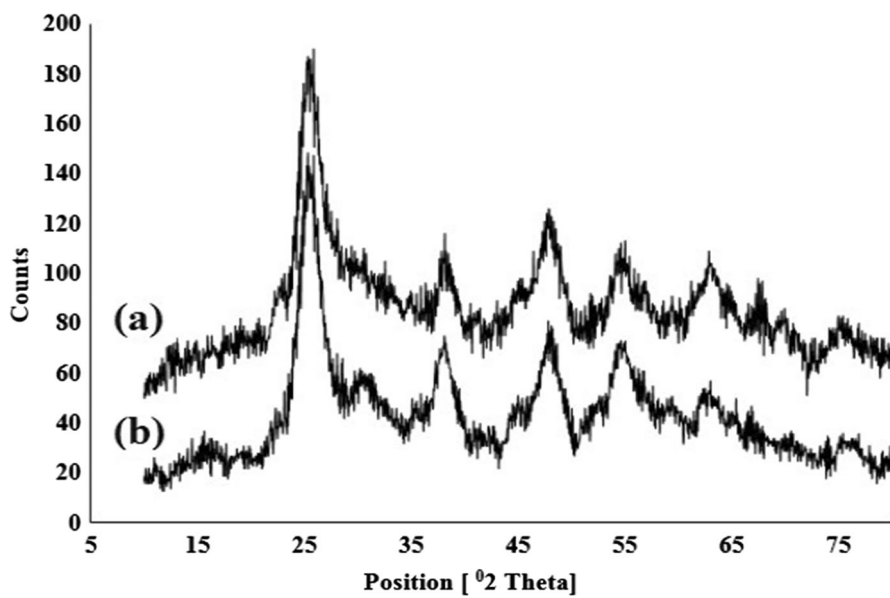


Fig. 3 X-ray diffraction patterns of TiO₂ (a) and TiO₂/RGO (b)

existence of anatase phase as the major phase [35]. Crystalline phase of TiO₂ nanoparticles was nearly unchanged after modification by reduced graphene oxide. Apart from two soft peaks at 2 θ : 15° and 30° in TiO₂/RGO XRD pattern, there are slight difference between (a) and (b) in shape and position of the diffraction peaks, which can be due to low amount of added RGO [36].

Photocatalytic degradation experiments

Generally, in order to evaluate the photocatalytic activity of the photocatalysts, degradation of RhB and MB were measured in aqueous solution. All the photocatalytic removal processes were carried out at room temperature and UV irradiation were provided by a 15 W mercury lamp, with wave length of 253 nm (Philips, Holland). The light source was positioned on top of the solutions and all the samples were irradiated under continuous stirring. In each experiment, in order to reach the adsorption equilibrium, the solutions were kept in the dark for half an hour before irradiation. The degradation efficiency was calculated by the following equation:

$$\text{Degradation efficiency} = \left(\frac{C_0 - C}{C_0} \right) \times 100$$

Here C_0 is the initial concentration of dye and C is the concentration at desired time. All concentration values were obtained by the maximum absorption at 550 nm and 664 nm for rhodamine B and methylene blue in the absorption spectrum.

Effect of different parameters in degradation process

Effect of RGO and PMMA ratio in composites for dye degradation

In order to get optimum ratio in composites, different samples of TiO₂/RGO (1/40, 1/60, 1/80, 1/100, 1/120, 1/140, 1/160, 1/180 w/w, a fixed amount of reduced graphene oxide was added to varied amount of titanium dioxide nano particles) and TiO₂/RGO/PMMA composites (1/40, 1/60, 1/80, 1/100, 1/120, 1/140, 1/160, 1/180 w/w, a fixed amount of prepared TiO₂/RGO were added to varied amount of poly (methyl methacrylate) were added to RhB solution (100 mL, 3 mg L⁻¹).

The proposed mechanism is shown in Fig. 4, RGO has no photocatalytic activity and photocatalytic reaction occurs due to titanium dioxide existence. UV irradiation, excites titanium dioxide nano particles, after oxygen insertion, radical intermediate species are formed, which are responsible for degradation. Excess amount of RGO covers titanium dioxide active surface and decreases photocatalytic activity of nano particles. The least degradation of the RhB dye occurs in the highest ratio of RGO (1/40), the best ratio revealed to be 1/80 and in lower amount of RGO, slight increase in degradation was observed. Increase in PMMA ratio both covers and shields nano particles surface against irradiation, and induces more aggregation which will lead to more decrease in dye degradation (Figs. S5 and S6).

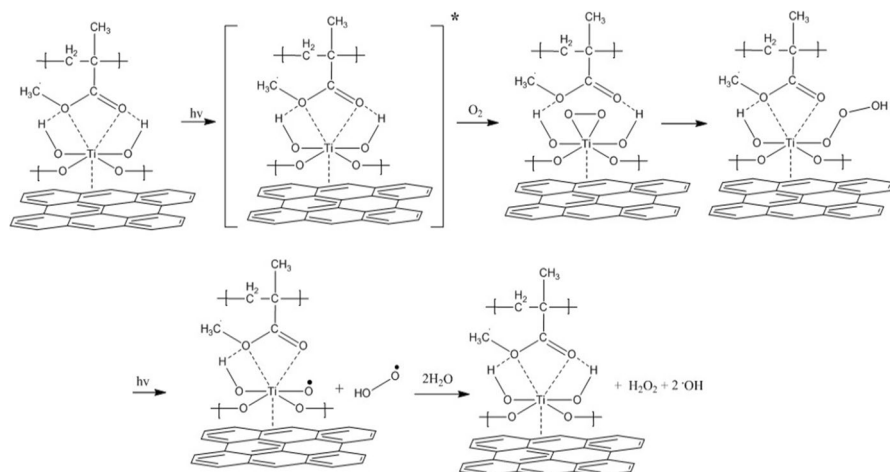


Fig. 4 Proposed mechanism of UV irradiation of titanium dioxide

Initial dye concentration and photocatalyst dosage effect

To examine initial concentration effect, 100 mL of RhB solution in desired concentrations (varying from 2 to 8 mg L⁻¹) were taken in a 250 mL beaker, and 1 g L⁻¹ of solid TiO₂ catalyst was added into the solution and shaken for half an hour in dark. In order to determine degradation efficiency, after specific time intervals, about 2 mL of dye solution were taken out, centrifuged and concentration of the dyes were analyzed by UV–VIS spectrophotometry afterwards (Fig. S7). The same procedure was conducted to determine optimum initial concentration for methylene blue.

The effect of photocatalyst dosage in the range of 0.5–2.5 g L⁻¹ in RhB degradation was also investigated (Fig. S7 inset). Increase in photocatalyst dosage from 0.5 to 1 g L⁻¹ resulted in tangible increase in degradation, while in higher catalyst dosage, boosting in degradation efficiency was not observed, thus 1 g L⁻¹ was set as photocatalyst dosage in the degradation experiments.

Time effect in RhB and MB degradation

Figs. 5 and 6 show the degradation rate of RhB and MB without photocatalyst and using different prepared photocatalysts. In the presence of no catalysts, when dye solutions are just UV irradiated, almost no degradation occurs. When dye solution is stirred in the presence of photocatalyst under no irradiation (in the dark), due to adsorption, decrease in dye concentration occurs. For instance, stirring the RhB solution for 10 min in the dark led to 13.5% decrease and in around 80 min, it increased to 26% (Fig. 5). Accordingly, for MB degradation (Fig. 6), after 10 min and 80 min 16.3% and 25.1% decrease were observed. Stirring continued to ensure equilibrium is occurred and no more dye will be absorbed. In the same time, when solutions were irradiated increase in degradation were noticeable.

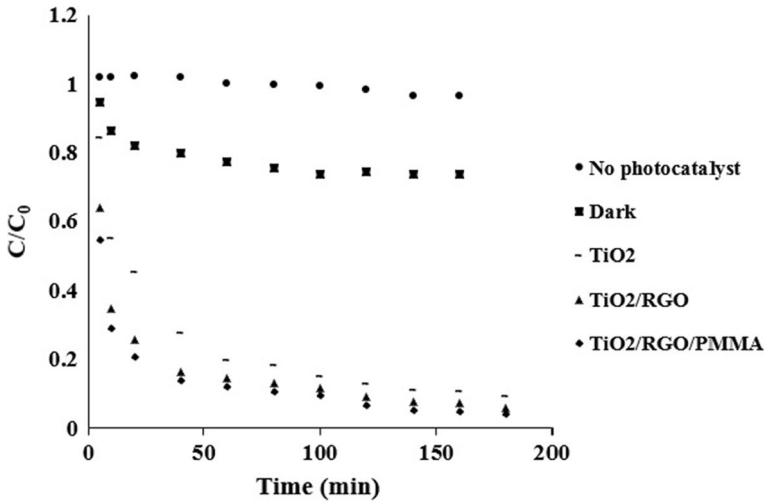


Fig. 5 Residual concentration (C/C_0) vs. time of RhB degradation (100 mL of 3 mg/L dye solution, photocatalyst dosage: 1 g/L)

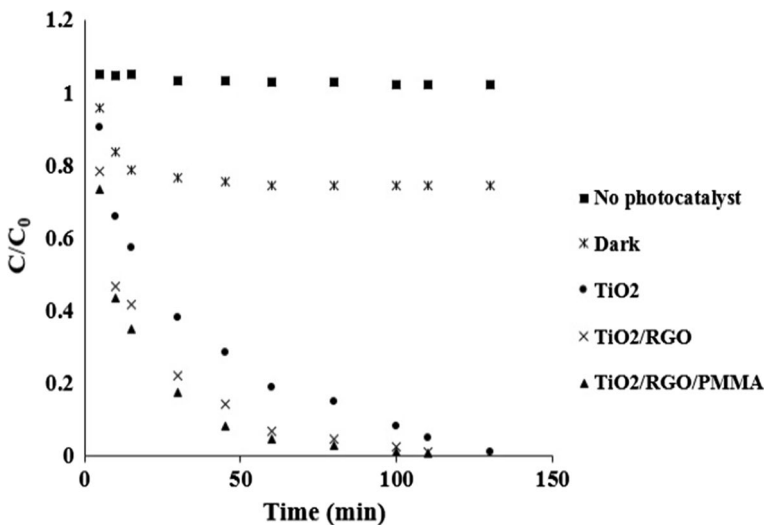
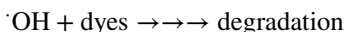
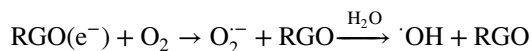
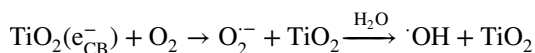
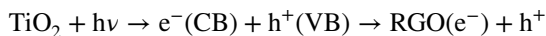


Fig. 6 Residual concentration (C/C_0) vs. time of MB dye degradation (100 mL of 5 mg/L dye solution, photocatalyst dosage: 1 g/L)

In other words it can be suggested that the photocatalytic process was primarily responsible for RhB and MB degradation and presence of both catalyst and UV light are indispensable for an effective degradation. After irradiation of 60 min, the degradation efficiency of RhB and MB is found to be 80% and 83% for pristine titanium dioxide, while in TiO₂/RGO there is an increase in degradation rate. Generally, graphene can act as an acceptor of the photo generated electrons. UV irradiation

of TiO_2 , excites electrons from valence bond to conduction band, electrons flow toward the graphene sheets, delocalization of electrons suppress recombination of electron–hole pair and improves photocatalytic performance (the process is shown in the following equations):



As presented in the time effect diagrams, the degradation of RhB and MB under UV light increases in the order of $\text{TiO}_2 < \text{TiO}_2/\text{RGO} < \text{TiO}_2/\text{RGO}/\text{PMMA}$.

PMMA existence made slight increase in degradation (as it can be deduced from the diagrams in Figs. 5 and 6), in other words, due to a minor increase in the degradation efficiency in the presence of $\text{TiO}_2/\text{RGO}/\text{PMMA}$ in comparison to TiO_2/RGO , it can be concluded that PMMA does not have crucial role in improving degradation and act as something like paste, but it was observed that the recovery of photocatalyst by centrifugation was faster and easier in the presence of PMMA degradation efficiency by TiO_2/RGO for RhB after 20, 80 and 140 min were 0.74, 0.86 and 0.92 while in the same times for $\text{TiO}_2/\text{RGO}/\text{PMMA}$, the degradation efficiencies were 0.79, 0.89 and 0.94.

Rhodamine B and methylene blue both have vivid peaks in 550 nm and 664 nm. (Due to some noises below 300 nm, starting wave length in RhB (Fig. 7a) was set at 300 nm) so the color change in dyes solution were readily monitored using UV–VIS spectrophotometer (Fig. 7). The decrease of absorbance value of the samples at λ_{max}

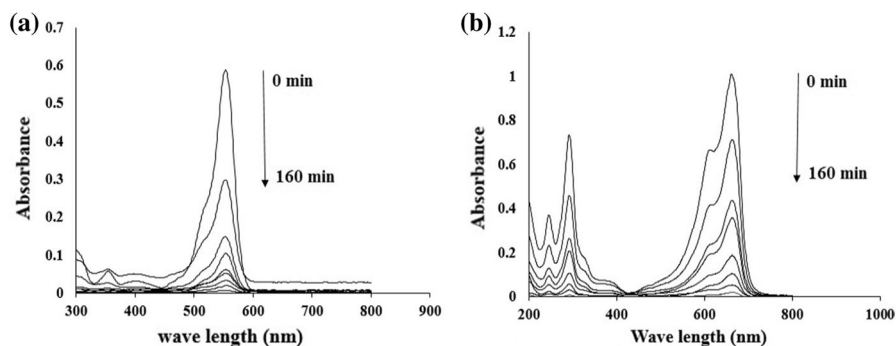


Fig. 7 Absorption versus wave length of RhB (100 mL of 3 mg/L dye solution, photocatalyst dosage: 1 g/L) (a) and MB (100 mL of 5 mg/L dye solution, photocatalyst dosage: 1 g/L) (b) in varied irradiation time in the presence of $\text{TiO}_2/\text{RGO}/\text{PMMA}$ composite

of the dyes, after irradiation in different time intervals indicates the rate of decolorization and photocatalyst activity under illumination.

The kinetics of the photocatalytic degradation rate of most organic compounds is described by pseudo-first order kinetics:

$$-\frac{dc(t)}{dt} = k_{app}c(t)$$

Here t is time, C is the concentration, and k_{app} is the apparent rate constant. By integrating the above mentioned equation with the initial condition $C(0)=C_0$, the following equation could be obtained:

$$\ln\left(\frac{c}{c_0}\right) = -k_{app}t$$

Kinetic analysis based on the pseudo first-order reaction for photocatalytic degradation of the dyes at optimum conditions were conducted, a plot of $\ln(C_0/C)$ versus the irradiation time (t) is reported in Figs. S8 and S9 for RhB and MB, respectively. The linear plot confirms that degradation of dyes by the prepared photocatalysts follow the pseudo-first order.

Photocatalyst reusability

Fig. S10 indicates the results of RhB degradation (100 mL of 3 mg/L dye, 1 g/L photocatalyst) under UV-C irradiation by $\text{TiO}_2/\text{RGO}/\text{PMMA}$ composite nano composite. After desired time, the photocatalyst was separated, washed and used for subsequent run. No noticeable loss in photo degradation was observed after three cycles, suggesting that the photocatalyst is stable during the photocatalytic reactions.

Conclusion

In summary, $\text{TiO}_2/\text{RGO}/\text{PMMA}$ nano composite (photocatalyst) was synthesized. TiO_2 nanoparticles were prepared by electrochemical method and the composites with reduced graphene oxide was conducted by the help of sonication. Composites were characterized by various techniques including XRD, FTIR, TEM, FESEM, and EDS. X-ray diffraction patterns confirmed existence of anatase as the main phase of the TiO_2 nanoparticles. In order to get better insight of TiO_2 morphology and size, TEM images of TiO_2 nanoparticles were prepared which confirmed spherical and uniformed shape of nanoparticles. EDS analysis were applied for monitoring characteristics peaks of titanium and carbon in native titanium dioxide and composites.

In order to evaluate photocatalytic activity of the composites, decolorization of two common dyes naming RhB and MB were tested in aqueous medium. Although PMMA adding did not resulted in tangible increase in dye degradation, it helped to easier recovery and shorter centrifuge time. Degradations were tested with different composites and the best results were obtained by the final composite ($\text{TiO}_2/\text{RGO}/$

PMMA) under UV illumination. The photocatalyst also revealed no noticeable loss in photo degradation after four cycles.

Acknowledgement The authors gratefully thank University of Zanjan for financial supports.

References

1. Bharathi KS, Ramesh ST (2013) Removal of dyes using agricultural waste as low-cost adsorbents: a review. *Appl Water Sci* 3:773–790
2. Merouani S, Hamdaoui O, Saoudi F, Chiha M (2010) Sonochemical degradation of Rhodamine B in aqueous phase: effects of additives. *Chem Eng J* 158:550–557
3. Boczkaj G, Fernandes A (2017) Wastewater treatment by means of advanced oxidation processes at basic pH conditions: a review. *Chem Eng J* 320:608–633
4. Dewil R, Mantzavinos D, Poullos I, Rodrigo MA (2017) New perspectives for advanced oxidation processes. *J Environ Manag* 195:93–99
5. Kamalan Kirubakaran AM, Selvaraj M, Maruthan K, Jeyakumar D (2012) Synthesis and characterization of nanosized titanium dioxide and silicon dioxide for corrosion resistance applications. *J Coat Technol Res* 9:163–170
6. Saeed M, Muneer M, Mumtaz N, Siddique M, Akram N (2018) Ag-Co₃O₄: Synthesis, characterization and evaluation of its photo-catalytic activity towards degradation of rhodamine B dye in aqueous medium. *Chin J Chem Eng* 26:1264–1269
7. Fuentes KM, Betancourt P, Marrero S, García S (2017) Photocatalytic degradation of phenol using doped titania supported on photonic SiO₂ spheres. *Reac Kinet Mech Cat* 120:403–415
8. Castellanos NJ, Martínez Rojas Z, Camargo HA, Biswas S, Granados-Oliveros G (2019) Congo red decomposition by photocatalytic formation of hydroxyl radicals (·OH) using titanium metal–organic frameworks. *Transit Met Chem* 44:77–87
9. Carević MV, Abazović ND, Savić TD, Novaković TB, Pjević DJ, Čomor MI (2018) Binary oxide ceramics for enhanced phenols degradation under simulated Solar light. *J Am Ceram Soc* 101(4):1420–1431
10. Prasai B, Cai B, Underwood MK, Lewis JP, Drabold DA (2012) Properties of amorphous and crystalline titanium dioxide from first principles. *J Mater Sci* 47:7515–7521
11. Alzamani M, Shokuhfar M, Eghdam E, Mastali S (2013) Influence of catalyst on structural and morphological properties of TiO₂ nanostructured films prepared by sol–gel on glass. *Prog Nat Sci Mater Int* 23:77–84
12. Martínez C, Canle LM, Fernández MI, Santaballa JA, Faria J (2011) Kinetics and mechanism of aqueous degradation of carbamazepine by heterogeneous photocatalysis using nanocrystalline TiO₂, ZnO and multi-walled carbon nanotubes–anatase composites. *Appl Catal B* 102:563–571
13. Ghasemi M, Amoozadeh A, Kowsari E (2017) Chitosan-functionalized nano-titanium dioxide: a novel and highly efficient nanocatalyst for the synthesis of 2,4,5-trisubstituted imidazoles under solvent-free conditions. *Reac Kinet Mech Cat* 120:605–617
14. Binas V, Venieri D, Kotzias D, Kiriakidis G (2017) Modified TiO₂ based photocatalysts for improved air and health quality. *J Materiomics* 3:3–16
15. Zhang D (2010) Enhanced photocatalytic activity for titanium dioxide by co-modification with copper and iron. *Transit Met Chem* 35:933–938
16. Than LD, Luong NS, Ngo VD, Tien NM, Dung TN, Nghia NM (2017) Highly visible light activity of nitrogen doped TiO₂ prepared by sol-gel approach. *J Electron Mater* 46:158–166
17. de Luna MDG, Lin JCT, Gotostos MJN, Lu MC (2016) Photocatalytic oxidation of acetaminophen using carbon self-doped titanium dioxide. *Sustain Environ Res* 26:161–167
18. Andoshe DM, Yim K, Sohn W (2018) One-pot synthesis of sulfur and nitrogen codoped titanium dioxide nanorod arrays for superior photoelectrochemical water oxidation. *Appl Catal B* 234:213–222
19. Song G, Chu Z, Jin W (2015) Enhanced performance of g-C₃N₄/TiO₂ photocatalysts for degradation of organic pollutants under visible light. *Chin J Chem Eng* 23:1326–1334
20. Yadav HM, Kim JS (2016) Solvothermal synthesis of anatase TiO₂-graphene oxide nanocomposites and their photocatalytic performance. *J Alloys Compd* 688:123–129

21. Jo WK, Kumar S, Isaacs MA, Lee AF, Karthikeyan S (2017) Cobalt promoted TiO₂/GO for the photocatalytic degradation of oxytetracycline and Congo Red. *Appl Catal B* 201:159–168
22. Liu S, Sun H, Liu S, Wang S (2013) Graphene facilitated visible light photodegradation of methylene blue over titanium dioxide photocatalysts. *Chem Eng J* 214:298–303
23. Wang D, Li X, Chen J, Tao X (2012) Enhanced photoelectrocatalytic activity of reduced graphene oxide/TiO₂ composite films for dye degradation. *Chem Eng J* 198–199:547–554
24. Alamelu K, Raja V, Shiamala L, Jaffar Ali BM (2018) Biphasic TiO₂ nanoparticles decorated graphene nanosheets for visible light driven photocatalytic degradation of organic dyes. *Appl Surf Sci* 430:145–154
25. Brindha A, Sivakumar T (2017) Visible active N, S co-doped TiO₂/graphene photocatalysts for the degradation of hazardous dyes. *J Photochem Photobiol A* 340:146–156
26. Roşu M-C, Socaci C, Floare-Avram V, Borodi G, Pogăcean F, Coroş M (2016) Photocatalytic performance of graphene/TiO₂-Ag composites on amaranth dye degradation. *Mater Chem Phys* 179:232–241
27. Klaysri R, Wichaidit S, Piticharoenphun S, Mekasuwandumrong O, Praserttham P (2016) Synthesis of TiO₂-grafted onto PMMA film via ATRP: using monomer as a coupling agent and reusability in photocatalytic application. *Mater Res Bull* 83:640–648
28. Cantarella M, Sanz R, Buccheri MA, Ruffino F, Rappazzo G, Scalese S (2016) Immobilization of nanomaterials in PMMA composites for photocatalytic removal of dyes, phenols and bacteria from water. *J Photochem Photobiol A* 321:1–11
29. Raliya R, Avery C, Chakrabarti S, Biswas P (2017) Photocatalytic degradation of methyl orange dye by pristine titanium dioxide, zinc oxide, and graphene oxide nanostructures and their composites under visible light irradiation. *Appl Nanosci* 7:253–259
30. Cantarella M, Sanz R, Buccheri MA, Romano L, Privitera V (2016) PMMA/TiO₂ nanotubes composites for photocatalytic removal of organic compounds and bacteria from water. *Mater Sci Semicond Process* 42:58–61
31. Gunpath U, Le H, Handy R, Tredwin C (2018) Anodised TiO₂ nanotubes as a scaffold for antibacterial silver nanoparticles on titanium implants. *Mater Sci Eng C* 91:638–644
32. Yuan XZ, Sergio P, Emanuele T, Giuliano G, Franco C, Vittorio M (2013) The exfoliation of graphene in liquids by electrochemical, chemical, and sonication-assisted techniques: a nanoscale study. *Adv Funct Mater* 23(37):4684–4693
33. Atchudan R, Jebakumar Immanuel Edison TN, Perumal S, Karthikeyan D, Lee YR (2017) Effective photocatalytic degradation of anthropogenic dyes using graphene oxide grafting titanium dioxide nanoparticles under UV-light irradiation. *J Photochem Photobiol A* 333:92–104
34. Venkatachalam N, Palanichamy M, Murugesan V (2007) Sol-gel preparation and characterization of alkaline earth metal doped nano TiO₂: efficient photocatalytic degradation of 4-chlorophenol. *J Mol Catal A* 273:177–185
35. Cheong YL, Yam FK, Ooi YW, Hassan Z (2014) Room-temperature synthesis of nanocrystalline titanium dioxide via electrochemical anodization. *Mater Sci Semicond Process* 26:130–136
36. Nguyen-Phan TD, Pham VH, Shin EW, Pham HD, Kim S, Chung JS (2011) The role of graphene oxide content on the adsorption-enhanced photocatalysis of titanium dioxide/graphene oxide composites. *Chem Eng J* 170:226–232

Publisher's Note Springer Nature remains neutral with regard to jurisdictional claims in published maps and institutional affiliations.